RESEARCH ARTICLE

Mechanism of delayed encephalopathy after acute carbon monoxide poisoning

Yan-Qing Huang, Zheng-Rong Peng*, Fang-Ling Huang, A-Li Yang
Department of Hyperbaric Oxygen, Xiangya Hospital, Central South University, Changsha, Hunan Province, China

Graphical Abstract

LINGO-1/NgR/p75^{NTR} regulates the downstream RhoA/ROCK2 signaling pathway, and LINGO-1 can be inhibited by retinoic acid (RA)

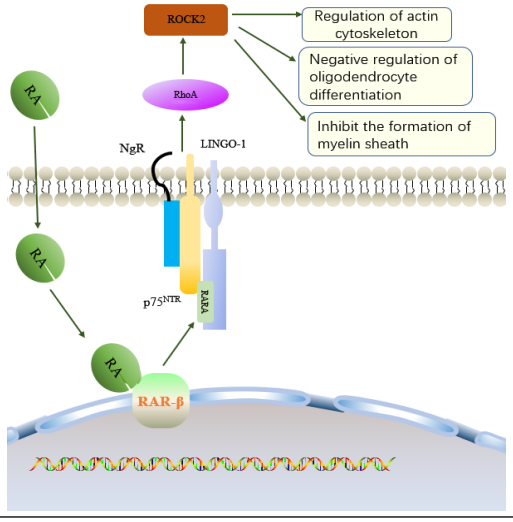

*Correspondence to:
Zheng-Rong Peng, PhD,
13873151139@163.com.

orcid:
0000-0003-3048-4344
(Zheng-Rong Peng)

doi: 10.4103/1673-5374.284995

Received: December 11, 2019
Peer review started: December 17, 2019
Accepted: March 4, 2020
Published online: June 19, 2020

Abstract

Many hypotheses exist regarding the mechanism underlying delayed encephalopathy after acute carbon monoxide poisoning (DEACMP), including the inflammation and immune-mediated damage hypothesis and the cellular apoptosis and direct neuronal toxicity hypothesis; however, no existing hypothesis provides a satisfactory explanation for the complex clinical processes observed in DEACMP. Leucine-rich repeat and immunoglobulin-like domain-containing protein-1 (LINGO-1) activates the Ras homolog gene family member A (RhoA)/Rho-associated coiled-coil containing protein kinase 2 (ROCK2) signaling pathway, which negatively regulates oligodendrocyte myelination, axonal growth, and neuronal survival, causing myelin damage and participating in the pathophysiological processes associated with many central nervous system diseases. However, whether LINGO-1 is involved in DEACMP remains unclear. A DEACMP model was established in rats by allowing them to inhale 1000 ppm carbon monoxide gas for 40 minutes, followed by 3000 ppm carbon monoxide gas for an additional 20 minutes. The results showed that compared with control rats, DEACMP rats showed significantly increased water maze latency and increased protein and mRNA expression levels of LINGO-1, RhoA, and ROCK2 in the brain. Compared with normal rats, significant increases in injured neurons in the hippocampus and myelin sheath damage in the lateral geniculate body were observed in DEACMP rats. From days 1 to 21 after DEACMP, the intraperitoneal injection of retinoic acid (10 mg/kg), which can inhibit LINGO-1 expression, was able to improve the above changes observed in the DEACMP model. Therefore, the overexpression of LINGO-1 appeared to increase following carbon monoxide poisoning, activating the RhoA/ROCK2 signaling pathway, which may be an important pathophysiological mechanism underlying DEACMP. This study was reviewed and approved by the Medical Ethics Committee of Xiangya Hospital of Central South Hospital (approval No. 201612684) on December 26, 2016.

Key Words: *brain injury; cell death; central nervous system; factor; injury; model; pathways; rat*

Chinese Library Classification No. *R441; R749.6+3; R741*

Introduction

Acute carbon monoxide (CO) poisoning is one of the most common clinical emergencies (Weaver, 2009). Furthermore, delayed encephalopathy is the most serious complication associated with acute CO poisoning. Delayed encephalopathy after acute CO poisoning (DEACMP) is characterized by a series of neurological and psychiatric symptoms, including dementia and dysfunction of the pyramidal and extrapyramidal systems, after a period of normal or near-normal presentation in patients who experience CO poisoning regain consciousness (Betterman and Patel, 2014). A high incidence of DEACMP has been reported after CO poisoning, affecting approximately 50% of patients with severe CO poisoning (Han et al., 2007). DEACMP may be caused by secondary brain tissue damage, due to CO-mediated brain tissue hypoxia, oxygen-based free radicals, and membrane

peroxidation, instead of due to direct hypoxia-induced damage (Yanagiha et al., 2017). Many pathological and neuroimaging studies have demonstrated that bilateral, symmetrical, malacic lesions in the globus pallidus, extensive demyelination in the brain, and neuronal necrosis and apoptosis comprise the major pathological changes associated with DEACMP (Beppu, 2014). Currently, DEACMP treatments involve corresponding measures to restore damaged brain structures and functions, to the greatest possible extent. However, in clinical practice, the efficacy of DEACMP treatments is poor, and the mortality and disability rates remain high (Hu et al., 2011). Current research has focused on exploring the ischemia-hypoxia hypothesis, the inflammation and immune-mediated damage hypothesis, and mechanisms associated with cellular apoptosis and direct neuronal toxicity induced by CO. However, these mechanisms have not been able to provide a satisfactory explanation for the complex clinical processes observed in DEACMP (Rose et al., 2017; Lettow et al., 2018).

Leucine-rich repeat and immunoglobulin-like domain-containing protein 1 (Lingo-1) is an important neural growth inhibitory factor expressed in the neuro-regenerative microenvironment of the central nervous system (CNS) (Andrews and Fernandez-Enright, 2015). Haines and Rigby (Haines and Rigby, 2008) found that Lingo-1 is only expressed in the mature brain. Lingo-1 is a transmembrane protein, primarily present in neurons and oligodendrocytes in the CNS. Lingo-1 forms a Nogo complex receptor with Nogo receptor (NgR) and p75 neurotrophin receptor ($p75^{NTR}$) (NgR/$p75^{NTR}$/Lingo-1), which plays a role in the inhibition of axonal regeneration (Mi et al., 2013; Yang et al., 2017; Almutiri et al., 2018). The expression of Lingo-1 is upregulated following CNS injury, accompanied by nerve cell death. Andrews and Fernandez-Enright (2015) believe that Lingo-1 upregulation and cell death in the CNS injury microenvironment hinder nerve regeneration. Lingo-1 plays an important role in cell death, inflammatory reactions, and glial scar formation; a microenvironment that antagonizes Lingo-1 expression can promote nerve fiber regeneration and survival. Lingo-1 activates the Ras homolog gene family member A (RhoA)/Rho-associated coiled-coil containing protein kinase 2 (Rock2) signaling pathway, which negatively regulates oligodendrocyte myelination, axonal growth, and neuronal survival and participates in the pathophysiological processes of many CNS diseases (Andrews and Fernandez-Enright, 2015). RhoA is a small GTPase protein in the Rho family that plays a key role in the reorganization of the actin cytoskeleton, cell adhesion, migration, and cell differentiation. Rock2 is the effector of RhoA (Heasman and Ridley, 2008; Korol et al., 2016). Lingo-1 and the Rock2 signaling pathway are involved in many degenerative CNS diseases, such as Alzheimer's disease, multiple sclerosis, and optic nerve injury. The primary pathological changes associated with Rock2 activation include neuronal death, axonal degeneration, glial hyperplasia, and demyelination (Wu et al., 2018; Hanf et al., 2020; Quan et al., 2020). However, at present, no research exists regarding the mechanism through which Lingo-1 expression is upregulated by CO-induced brain damage. Therefore, this study focused on the relationship between CO-mediated brain injury and nerve growth inhibitory factors.

Retinoic acid (RA) is a vitamin A metabolite that is associated with various biological functions, including important roles in nervous system growth, development, and regeneration (Walker et al., 2018). Puttagunta and Di Giovanni (2011) found that the RA signaling pathway can directly inhibit the Nogo receptor (NgR)/Lingo-1 complex, both *in vivo* and *in vitro*, inducing axonal regeneration after middle cerebral artery occlusion in rat brains. In addition, Xing et al. (2015) found that Lingo-1 expression was upregulated in a cerebral ischemia rat model; however, this upregulated expression was inhibited by RA treatment, which also increased the number of synapses.

Currently, studies examining the effector mechanisms of Lingo-1 and the RhoA/Rock2 signaling pathway during DEACMP are lacking. Therefore, in this study, we used RA to inhibit Lingo-1 expression and aimed to perform a preliminary analysis of the regulatory mechanisms involving Lingo-1 and the RhoA/Rock2 signaling pathway in DEACMP-induced brain damage and to assess a possible novel therapy.

Materials and Methods

Animals

In total, 96 healthy, adult, specific-pathogen-free grade, male Sprague-Dawley rats (weighing 220–225 g, aged 5 weeks) were purchased from the Hunan SJA Laboratory Animal Co., Ltd., China (approval No. SCXK [Xiang] 2016-0002). After purchase, the animals were housed at the Department of Laboratory Animals, Central South University, with *ad libitum* access to food and water. All rats were fed separately, and maintained in a 12-hour light/dark cycle, with cage temperature at 21–22°C. The animal cages were also cleaned regularly. This study was reviewed and approved by the Medical Ethics Committee of Xiangya Hospital of Central South Hospital (approval No. 201612684), on December 26, 2016.

Basic training and screening with the Morris water maze test

All rats were trained and screened using the Morris water maze test (Sipos et al., 2007). The Morris water maze (Shenzhen Reward Life Science Co., Ltd., Shenzhen, Guangdong Province, China) consisted of a circular pool (diameter: 180 cm, height: 50 cm, water depth: 30 cm) and a camera that was connected to a computer. The circular pool was divided into four points (north, south, east, and west), and four quadrants along the central point (southeast, southwest, northeast, and northwest). The target platform was fixed in the northeast quadrant, 2 cm below the water surface. The water maze was maintained at 21–22°C, and noise and light interference were strictly controlled. Consistency in the arrangement of indoor objects and the surrounding environment was maintained. Milk was added to the pool to create an opaque liquid, and the rats were required to learn how to identify the location

of the hidden platform, based on the spatial cues around the pool. All rats were randomly numbered before undergoing 6 continuous days of water maze training, receiving one session per day, in the morning. At the start of the experiment, the rats were randomly placed into the water in one of the quadrants, facing the wall, and the timer was started. If the rat was able to locate the platform within 90 seconds, the time taken to climb the platform was recorded as the escape latency. After the rat reached the platform, it was allowed to remain there for 10 seconds. If the rat was unable to find the platform within 90 seconds, the researcher would guide the rat to the platform and allow it to remain there for 10 seconds, to strengthen its memory of the platform, and the time taken to locate the platform was recorded as 90 seconds. The rats were placed in each quadrant, in sequence, during the experiment, and the mean escape latency for all four quadrants was calculated. After the experiment, a dry towel was used to dry the rat before returning it to the cage. The results recorded on day 6 were used as the baseline result, and any rats that were unable to locate the platform within 90 seconds were predetermined to be eliminated from the study; however, none were eliminated in this study.

Group management

The 96 rats that successfully completed basic water maze training were randomized into control (normal rats), DEACMP, and RA + DEACMP groups, containing 32 rats in each group. Within each group, the 32 rats were randomly and equally divided into four subgroups, based on time points 3, 7, 14, and 21 days. Then, four rats in each subgroup were randomly selected for immunohistochemical analysis, myelin sheath staining, Nissl staining, and hematoxylin and eosin staining, whereas the remaining four rats were used to perform quantitative real-time polymerase chain reactions.

Establishment of the rat DEACMP model

The CO inhalation method, reported by Thom et al. (2004) and Xue et al. (2017), was used to create the DEACMP model. Briefly, the rats in the DEACMP and RA + DEACMP groups were placed in seven transparent boxes and forced to inhale 1000 ppm CO gas (Changsha Zhanyuan Gas Co. Ltd., Changsha, Hunan Province, China), for 40 minutes, followed by the inhalation of 3000 ppm CO gas, for the next 20 minutes. After the rats lost consciousness, they were removed from the boxes and allowed to recover consciousness in fresh air. The CO concentrations were monitored using a CO sensor (Edkors Co., Ltd., Changsha, Hunan Province, China). The rats in the control group were placed in the aforementioned transparent boxes, containing normal air, for approximately the same duration as the rats in the DEACMP and RA + DEACMP groups.

The criteria outlined by Liu et al. (2002) were used to determine the successful establishment of the DEACMP model. The specific criteria were as follows. (i) Toxicity presentation in the animals: 15 minutes after the initiation, the rats become active and excitable. Subsequently, the rats presented indications of shortness of breath and heavy breathing, and their ears, paws, and tails appeared cherry-red in color. After 40 minutes, the rats exhibited mania and began to bang the sides of the cages. The rats then showed signs of limb paralysis and lost consciousness. (ii) Carboxyhemoglobin (COHb) quantitation: a blood COHb level > 50% is indicative of CO poisoning. (iii) Water maze test (performed 1 day after model construction): The rats displayed cognitive impairments, determined by an increase in the escape latency.

Determination of blood COHb

Blood was collected from the tail vein, and the modified, dual-wavelength COHb quantitation method (Sakata et al., 1983) was used to measure the blood COHb concentrations. First, 0.1 mL of rat tail-vein blood was added to 20 mL of 0.4 M ammonium hydroxide and mixed evenly, followed by the addition of 20 mg sodium dithionite, mixed evenly. A microplate reader (Tecan, Shanghai, China) was then used to measure the absorbances (A) at 535 and 578 nm, over 10 minutes. The blood COHb level was then calculated using the following formula: $\text{COHb}\ (\%) = (2.44 \times A_{535\ \text{nm}}/A_{578\ \text{nm}} - 2.68) \times 100$.

RA intervention

RA (Changsha Boyi Co., Ltd., Changsha, Hunan Province, China) was dissolved in dimethyl sulfoxide [Sigma-Aldrich (Shanghai) Trading Co., Ltd., Shanghai, China], to form a 3 mg/mL solution. RA solution (10 mg/kg) was administered to the rats in the RA group every day, by intraperitoneal injection, starting from day 1 to day 21 after the DEACMP model construction (Xing et al., 2015). A 10 mg/kg dimethyl sulfoxide solution was administered to the rats in the DEACMP and control groups, through daily intraperitoneal injections.

Morris water maze test

The Morris water maze experiment was performed on days 3, 7, 14, and 21 after DEACMP model construction in rats, using the same methods described for basic training.

Tissue sample collection

After the rats underwent the water maze experiment, 10% chloral hydrate was administered via intraperitoneal injection (0.4 mL/kg) for anesthesia. After the induction of anesthesia, the rats were placed in the supine position, and the chest was fully opened, to expose the heart. A syringe needle was introduced through the left ventricle, into the ascending aorta. Simultaneously, the abdominal aorta was clamped with hemostats, and the right auricle appendage was excised.

To examine brain morphology and protein immunopositivity, the rats were rapidly perfused with physiological saline, until the eyeballs and paws turned white. Subsequently, the rats were perfused with 4% paraformaldehyde, until opisthotonos occurred and the head became rigid. After the skull was opened and the whole brain was dissected, the cerebellum was removed. After paraformaldehyde fixation for 24 hours, the brain tissues were embedded in paraffin, and continuous sections of approximately 4-μm thickness were cut using a microtome.

To test the expression of target genes, a total of 100 mL

4% physiological saline was rapidly infused into the rats and then the rats were decapitated and the skulls were opened, to allow the removal of the brain. The brain tissues were placed in a diethyl pyrocarbonate-treated culture dish, at which point the cerebellum was removed. The tissues were placed in sterile cryotubes, and liquid nitrogen was added before the tubes were transferred to a freezer, for storage at –80°C.

Hematoxylin and eosin staining

The paraffin sections were dewaxed, hydrated and stained with hematoxylin and eosin (Wuhan Servicebio Technology Co., Ltd., Wuhan, Hubei Province, China). Then, the slices were washed with distilled water, dehydrated with an alcohol gradient, and treated with xylene to induce transparency, according to the manufacturer's protocol (Li et al., 2020). Pathological changes in the hippocampus were observed using an optical microscope (Carl Zeiss AG, Baden-Württemberg, Germany), under 400× magnification, and images were collected to observe the morphologic variations of neurons in the hippocampus.

Myelin staining

The paraffin sections were dewaxed until hydrated and preheated in Luxol fast blue (LFB) (Wuhan Servicebio Technology Co., Ltd.) in an oven at 60°C for 30 minutes. The sections were immersed in the dye for 3 hours, followed by 10 minutes of cooling and rinsing with tap water. The sections were then alternately immersed in 70% ethanol and lithium carbonate solutions for differentiation before terminating the reaction using tap water. The degree of differentiation in each section was controlled under the microscope (determination of the degree of differentiation: myelin sheath is blue and the background is colorless). The slices were then dehydrated in absolute alcohol, and treated with xylene to induce transparency, followed by encapsulation with neutral resin, according to the manufacturer's protocol (Ma et al., 2019). Myelin sheath damage at the lateral geniculate body was observed under an optical microscope, at 400× magnification, and images were acquired to observe optical density changes in the myelin sheaths of neurons.

Nissl staining (toluidine blue staining)

The paraffin sections were dewaxed until hydrated, followed by a 10-minute toluidine blue staining (Wuhan Servicebio Technology Co., Ltd.) and differentiation in 95% alcohol (brain tissues are differentiated until the Nissl bodies appear deep blue and the background becomes pale blue or colorless). The sections were air-dried, cleared, and then mounted with neutral resin. Morphological changes in the hippocampal neurons were observed under an optical microscope at 400× magnification. Four randomly selected, non-overlapping regions were selected from the images, and an average value was taken for the number of Nissl positive cells.

Immunohistochemical staining

The paraffin sections were dewaxed, hydrated, repaired with citric acid buffer (1 M, pH 6.0, Wuhan Servicebio Technology Co., Ltd.), and incubated overnight at 4°C in primary antibody (rabbit anti-Lingo-1 polyclonal antibodies, 1:100, Bioss Antibodies Co., Ltd., Beijing, China; rabbit anti-RhoA polyclonal antibodies, 1:100, Affinity Inc., Cincinnati, OH, USA; rabbit anti-Rock2 polyclonal antibodies, 1:100, Affinity Inc.). Sections were incubated at 37°C for 2 hours with biotin-labeled rabbit anti-rat IgG (Boster Biological Technology Co., Ltd., Wuhan, Hubei Province, China), then washed with streptavidin-biotin complex (Boster Biological Technology Co., Ltd.). Then, the sections were stained by 3,3′-diaminobenzidine (Changsha Boyi Co., Ltd.). After dehydration, clearing, and mounting with neutral resin, the sections were observed by an optical microscope. Image-Pro Plus 6.0 software (Media Cybernetics, Inc., Rockville, MD, USA) was used to analyze the optical density.

Fluorescent quantitative real-time polymerase chain reaction

The TRIzol method (Turkseven et al., 2017) was used to extract total RNA from rat whole-brain tissues. After testing the concentration and purity of RNA using a Nanodrop 2000 (Thermo Fisher Scientific Co., Ltd.), the RNA was reverse transcribed into complementary DNA, using a reverse transcription kit (Wuhan Servicebio Technology Co., Ltd.) following the manufacturer's instructions. SYBR green-based quantitative real-time polymerase chain reaction was used to quantitate the mRNA expression levels of Lingo-1, Rock2, and RhoA, using glyceraldehyde 3-phosphate dehydrogenase as an internal reference. The primers were synthesized by Wuhan Servicebio Technology Co., Ltd. **Table 1** provides the primer sequences and amplification product sizes. The reaction conditions were as follows: 40 cycles of 95°C for 15 seconds and 60°C for 60 seconds. After the reaction ended, the Ct values of the samples were read by the fluorescence quantitative polymerase chain reaction machine (ABI Inc., Foster City, CA, USA), and the international relative quantitation method ($2^{-\Delta\Delta Ct}$) was used (Zhao et al., 2018). The final value of the target genes was expressed relative to the level of the internal reference gene.

Statistical analysis

Data are expressed as the mean ± standard deviation (SD). All data analyses were performed using the statistical software SPSS 20.0 (IBM SPSS Inc., Chicago, IL, USA) and GraphPad Prism 8 (GraphPad Software Inc., San Diego, CA, USA). One-way analysis of variance and the least significant difference test were used to compare statistical differences between groups. The Spearman test was used to perform correlation analysis between the expression of Lingo-1 protein and pathological changes. A P-value < 0.05 was considered significant.

Results

Quantitative analysis of experimental animals

In this study, none, two rats, and one rat died in the control, DEACMP, and RA + DEACMP groups, respectively. The unsuccessful induction of the DEACMP model was observed in two and three rats in the DEACMP and RA + DEACMP

Table 1 Primers for the fluorescent quantitative real-time polymerase chain reaction

Genes	Primer sequences	Product length size (bp)
Gapdh	F: 5′-CTG GAG AAA CCT GCC AAG TAT G-3′	138
	R: 5′-GGT GGA AGA ATG GGA GTT GCT-3′	
Lingo-1	F: 5′-TCA ACA TCA ATG CCA TAC GGG-3′	213
	R: 5′-AGG AAA GAT TGA GGA AAC GGA G-3′	
RhoA	F: 5′-TGT GGC AGA TAT TGA AGT GGA CG-3′	261
	R: 5′-CGC CTT GTG TGC TCA TCA TTC-3′	
Rock2	F: 5′-TGC TAT TGG ATA AAC ACG GAC A-3′	174
	R: 5′-ACC AAT CAC ATT CTC GTC CAT AG-3′	

F: Forward; GAPDH: glyceraldehyde 3-phosphate dehydrogenase; LINGO-1: leucine-rich repeat and immunoglobulin-like do-main-containing protein-1; R: reverse; RhoA: Ras homolog gene family member A; ROCK2: Rho-associated coiled-coil containing protein kinase 2.

groups, respectively. These animals were eliminated from the study. The eliminated animals were subsequently supplemented. During the RA treatment process, no animal deaths, side effects, or adverse reactions were observed. No manifestation was observed in the control group, suggesting the occurrence of poisoning or neurobehavioral cognitive impairment.

Effects of DEACMP model induction and RA treatment on Morris water maze results

The Morris water maze results showed significant differences in platform identification latency among the control, DEACMP, and RA + DEACMP groups, on days 7 and 14 ($P < 0.05$). Significantly increased latencies were observed in the DEACMP group on days 7 and 14 compared with those in the control group ($P < 0.05$). Reduced latencies were observed in the RA + DEACMP group compared with those in the DEACMP group, on days 7 and 14 ($P < 0.05$; **Figure 1**). Representative swimming paths are shown in **Figure 1A**. Therefore, the DEACMP model rats showed significantly impaired learning and memory abilities compared with the rats in the control group, and after intervention with RA, this impaired ability was improved.

Effects of DEACMP model induction and RA treatment on neuronal morphologies

Hematoxylin and eosin staining

Hematoxylin and eosin staining in the hippocampal area was used to observe the neurons 14 days after DEACMP model induction. The hippocampi of rats from the control group did not exhibit any apparent swelling, and the cells were arranged tightly, with normal morphologies. The neurons appeared round or oval, with intact nuclear membranes, and the nucleoli could be observed (**Figure 2A**). In the DEACMP group, large numbers of degraded and necrotic neurons could be observed, appearing as shrunken neuronal cell bodies, with gaps around indistinct, red-colored cells, with strongly eosin-stained cytoplasms. Their nucleoli appeared deeply-stained and deviated, with apparent pyknosis and cytoplasmic and nuclei condensation (**Figure 2B**). In the RA + DEACMP group, the neurons were arranged tightly, with occasional neuron degeneration observed in the hippocampi and few red-colored cells (**Figure 2C**).

Myelin staining

Myelin sheath staining in the lateral geniculate body was used to observe changes in the myelin sheaths of neurons, 14 days after DEACMP model induction. The myelin sheaths of neurons in the control group were uniformly stained deep blue, with an ordered arrangement and uniform thickness (**Figure 2D**). The myelin sheaths in the DEACMP group exhibited signs of degeneration and swelling, with pale staining, disordered arrangement, uneven thickness, and apparent demyelinating lesions (**Figure 2E**). In the RA + DEACMP group, no apparent swelling of the myelin sheath was observed, and the staining and arrangement were uniform, with a few demyelinating lesions observed (**Figure 2F**). **Figure 2** demonstrates that rats with acute CO exposure-induced brain damage suffer from demyelination changes, which can be alleviated by RA intervention. Similar data were observed for LFB staining (**Figure 2J**).

Nissl staining

Nissl staining in the hippocampal area was used to observe neurons 14 days after DEACMP model induction. In the control group, Nissl-stained sections displayed many deeply stained neurons, dense Nissl bodies, and deep, blue coloration (**Figure 2G**). In the DEACMP group, a significant reduction in the number of hippocampal neurons, the shrinkage or detachment of neuronal cell bodies, pyknosis, significant reductions or losses of Nissl bodies, and lighter blue coloration was observed (**Figure 2H**). In the RA + DEACMP group, the number of hippocampal neurons increased, along with some pyknosis. An increase in the number of Nissl bodies and a deeper blue coloration were also observed, compared with those in the DEACMP group (**Figure 2I**). **Figure 2** shows that rats with acute CO exposure-induced brain damage demonstrated Nissl cell changes, which could be alleviated by RA intervention. Similar data were observed when the numbers of Nissl-positive cells were quantified (**Figure 2K**).

Immunopositivity of Lingo-1, RhoA, and Rock2 in DEACMP rats

Figure 3 shows the detection of Lingo-1, RhoA, and Rock2 expression, appearing as yellow, brown, and deep brown, respectively. Axonal and myelin sheath injuries can be identified using myelin staining in the optic tract region of the lateral geniculate nucleus (Sun et al., 2014, 2015), and RhoA/Rock2 is expressed in various parts of the brain, including

the cortex, central nervous system, and basal ganglia (Yu et al., 2010; Wang et al., 2019). Therefore, to facilitate observations, Lingo-1 immunopositivity was detected in the lateral geniculate bodies, primarily in the nerve fibers, whereas RhoA immunopositivity was detected in the basal ganglia, primarily in the neuronal nuclei or cytoplasm and Rock2 immunopositivity was detected in the cortex, primarily in the neuronal nuclei or cytoplasm.

Immunohistochemical staining showed the immunopositivity of Lingo-1, RhoA, and Rock2, in the control, DEACMP, and RA + DEACMP groups, 14 days after DEACMP model induction (**Figure 3**). Compared with the control group, Lingo-1 immunopositivity in the nerve fibers of the DEACMP group was significantly increased, with a wider and longer distribution, and RhoA and Rock2 immunopositivity in the neurons significantly increased, with a dense distribution. In contrast, compared with the DEACMP group, Lingo-1 immunopositivity was reduced, with a thinner and shorter distribution, and the RhoA and Rock2 distributions were uniform, with decreased immunopositivity, in the RA + DEACMP group (**Figure 3**).

To determine the relationship between the neural growth inhibitory factor and pathological changes, we performed a correlation analysis between Lingo-1 protein immunopositivity and LFB staining, in the lateral geniculate bodies and Nissl-positive cells in the hippocampal region. The analysis revealed a negative correlation between the number of Nissl-positive cells and Lingo-1 immunopositivity ($r = –0.51$, $P = 0.043$). Additionally, a negative correlation was identified between the LFB-positive staining results and Lingo-1 immunopositivity ($r = –0.60$, $P = 0.013$; **Figure 4**).

Lingo-1, RhoA, and Rock2 gene expression in whole-brain samples from DEACMP rats

The differences in Lingo-1, RhoA, and Rock2 mRNA expression levels in whole-brain samples were evaluated among the control, DEACMP, and RA + DEACMP groups, on days 3, 7, 14, and 21 after DEACMP model induction, and significant differences were identified ($P < 0.05$; **Figure 5**). Lingo-1, RhoA, and Rock2 mRNA expression levels were significantly increased in the DEACMP group compared with those in the control group for all time points ($P < 0.05$; **Figure 5**). The Lingo-1 mRNA expression levels were reduced in the RA + DEACMP group compared with that in DEACMP group, and the inter-group differences were significant on days 3 and 7, whereas on days 14 and 21, differences were not obvious ($P < 0.05$; **Figure 5A**). The RhoA mRNA expression levels were significantly reduced in the RA + DEACMP group compared with those in the DEACMP group for all time points ($P < 0.05$; **Figure 5B**). The Rock2 mRNA expression levels were significantly reduced in the RA + DEACMP group compared with those in the DEACMP group on days 7, 14, and 21 ($P < 0.05$; **Figure 5C**).

Discussion

At present, the establishment of a DEACMP model, by CO inhalation poisoning, is consistent with the common clinical mode of CO poisoning. Experimental studies after CO poisoning have identified spatial learning and memory impairment, apoptosis in large numbers of nerve cells, and demyelination lesions (Dong et al., 2018; Zhao et al., 2018). In this study, the water maze experiment results revealed cognitive impairments in the DEACMP rats. Hematoxylin and eosin staining revealed that large numbers of neurons underwent apoptosis and necrosis in DEACMP rats. In addition, Nissl staining indicated the disappearance of Nissl bodies in many neurons, whereas myelin sheath staining revealed the swelling of the myelin sheath, discontinuous myelin sheaths, and demyelination lesions. Together, these results confirmed the existence of pathological changes and behavioral deficiencies following DEACMP-induced brain damage.

In the 1980s, researchers found that the CNS microenvironment is vital to the survival and regeneration of damaged nerves and that inhibitory factors in this microenvironment may play more important roles (Baldwin and Giger, 2015). After many years of neurological research, the current consensus is that the myelin sheath in the CNS is a major obstacle to neuroregeneration (Schwab, 2002). Andrews and Fernandez-Enright (2015) demonstrated that Lingo-1 plays an important role in the CNS injury microenvironment, hindering nerve regeneration.

Myelin sheath rupture after injury may generate more neural growth inhibitory factors, inhibiting neuronal axon re-generation and neuron survival. In recent years, several studies have reported that the etiology of DEACMP involves changes in demyelination. In addition, brain MRI scans, performed in patients, clearly indicated the demyelination of the bilateral periventricular junctions, which persisted for long periods of time (Hu et al., 2011). Therefore, we believe that the complex clinicopathological processes and poor prognoses associated with DEACMP are due to extensive demyelination and the production of large amounts of neural growth inhibitory factors. The CNS neuroregeneration microenvironment contains many neural growth inhibitors, among which Lingo-1 is one of the most important inhibitors (Mi et al., 2008). After CNS damage, Lingo-1 is selectively and highly expressed in neurons and oligodendrocyte precursor cells, and the inhibition of Lingo-1 expression can significantly promote the regeneration of myelin following CNS demyelinating lesions associated with multiple sclerosis (Youssef et al., 2019). In Alzheimer's disease model rats, an anti-Lingo-1 antibody was able to promote the regeneration of the myelin sheath (Youssef et al., 2019). Similarly, in a model of spinal cord injury, using a Lingo-1 polyclonal antibody to specifically block Lingo-1 activity was shown to significantly reduce RhoA activity, improving the survival rate of neurons, and Lingo-1 RNA interference treatment in neural stem cells was able to promote functional recovery after spinal cord injury (Lv et al., 2010; Youssef et al., 2019). In this study, we detected the high expression of Lingo-1 after CO exposure for the induction of a DEACMP model, suggesting that nerve injury following CO poisoning may be related to the high expression of Lingo-1. The correlation between Lingo-1 expression and pathological damage after CO

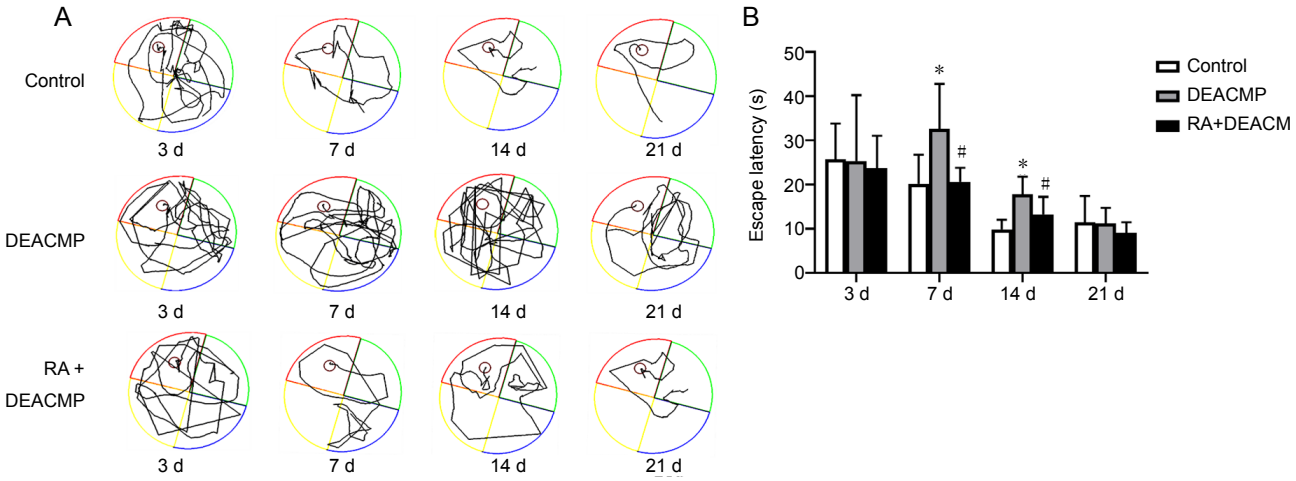

Figure 1 Behavior changes observed in rats with acute carbon monoxide exposure-induced brain damage.
(A) Morris water maze trajectory map for each group. The representative motion track from single animals in the DEACMP group was generally more complex than that in the control group. The representative motion track from single animals of the RA + DEACMP group was simpler than that in the DEACMP group. (B) Escape latencies for each group. Data are presented as the mean ± SD (n = 8). *P < 0.05, *vs.* control group; #P < 0.05, *vs.* DEACMP group (one-way analysis of variance followed by the least significant difference test). DEACMP: Delayed encephalopathy after acute carbon monoxide poisoning; RA: retinoic acid.

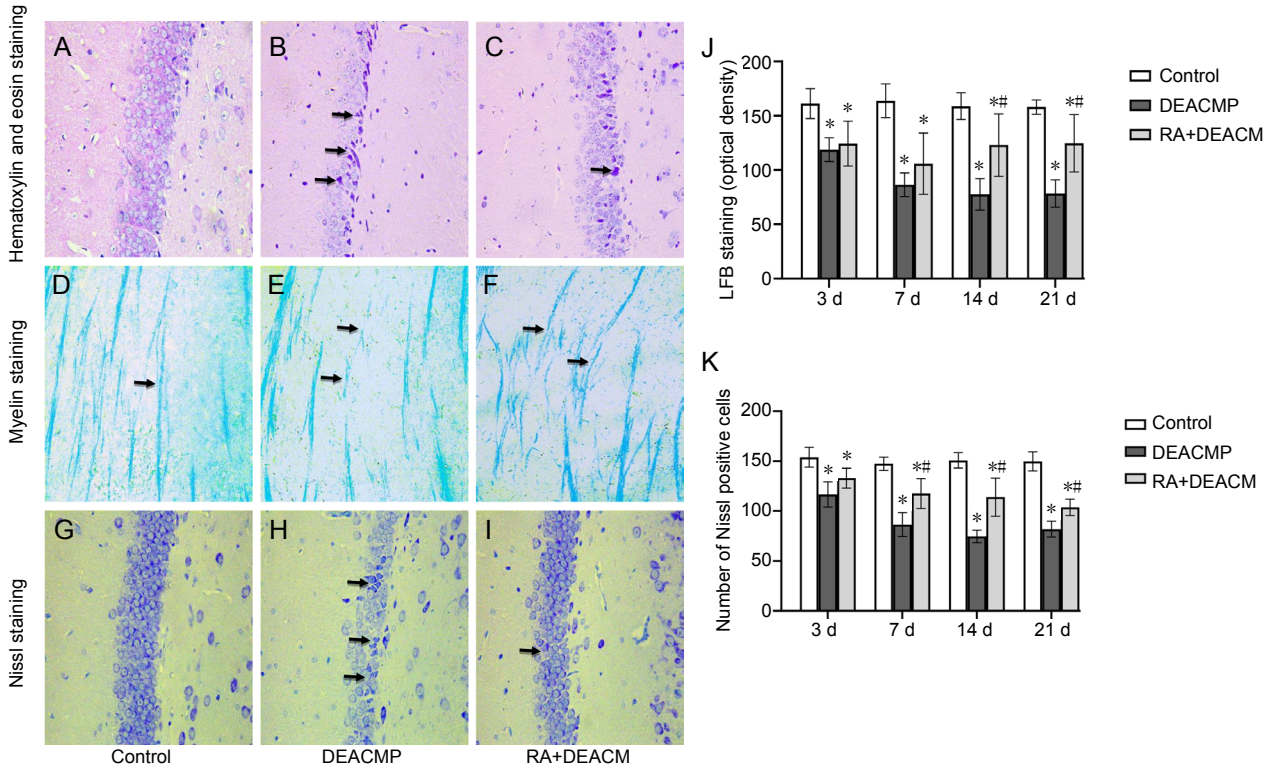

Figure 2 Effects of carbon monoxide exposure on morphological changes in the hippocampal region and the lateral geniculate body.
(A–I) Morphological images showing hematoxylin and eosin staining (A–C), myelin staining (D–F), and Nissl staining (G–I), 14 days after carbon monoxide exposure in the control (A, D, and G), DEACMP (B, E, and H), and RA + DEACMP (C, E, and I) groups (400× magnification). Compared with the control and RA + DEACMP groups, the numbers of denatured necrotic neurons and pyknotic Nissl bodies significantly increased in the DEACMP group. The changes in demyelination in the DEACMP group are also obvious. Black arrows in B and C indicate degraded and necrotic neurons; black arrows in D–F indicate the morphology of the neuronal myelin sheath; and black arrows in H and I indicate pyknosis Nissl bodies. (J) Luxol fast blue (LFB) staining. (K) The number of Nissl positive cells in 400× magnification field. Data are presented as the mean ± SD (n = 4). *P < 0.05, *vs.* control group; #P < 0.05, *vs.* DEACMP group (one-way analysis of variance followed by the least significant difference test). DEACMP: Delayed encephalopathy after acute carbon monoxide poi-soning; RA: retinoic acid.

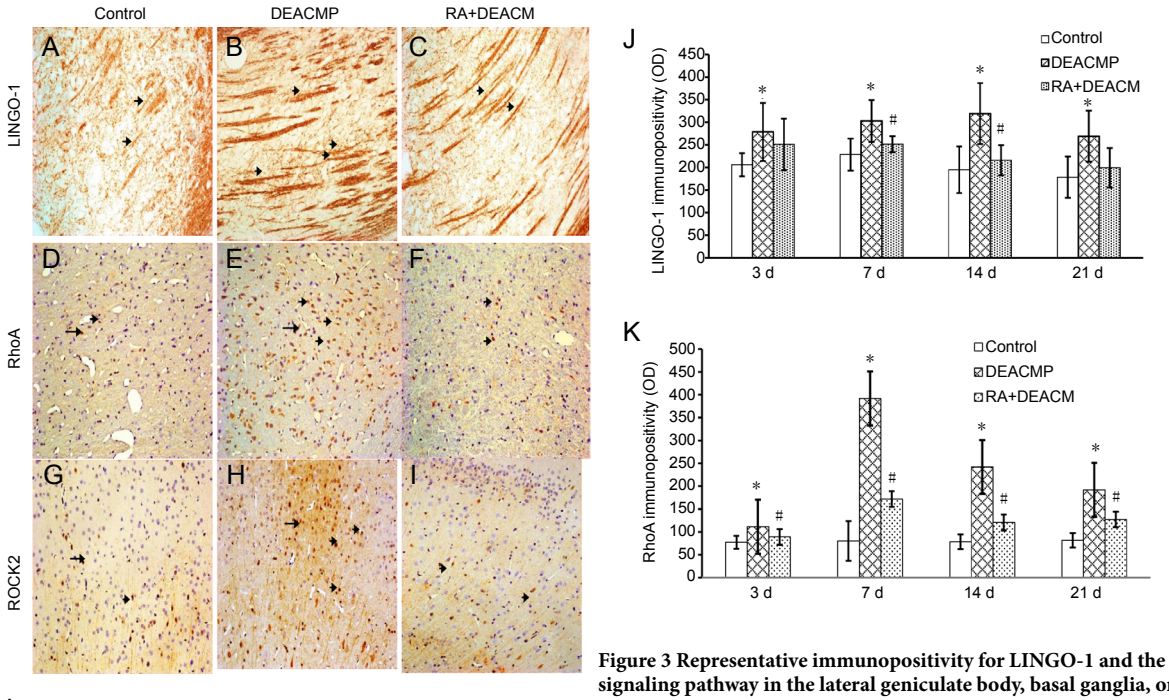

Figure 3 Representative immunopositivity for LINGO-1 and the RhoA/ROCK2 signaling pathway in the lateral geniculate body, basal ganglia, or cortex of DEACMP model rats at 14 days.

(A–I) Immunohistochemical staining for LINGO-1 (A–C), RhoA (D–F), and ROCK2 (G–I) in the control (A, D, and G), DEACMP (B, E, and H), and RA + DEACMP (C, F, and I) groups, 14 days after carbon monoxide exposure (400× magnification). Compared with the control and RA + DEACMP groups, LINGO-1, RhoA, and ROCK2 immunopositivity significantly increased in the DEACMP group. The black arrow indicates LINGO-1/RhoA/ROCK2 positive expression. Positive LINGO-1, RhoA, and ROCK2 stains appeared yellow, brown, and deep brown, respectively. (J–L) Quantitative results for LINGO-1 (J), RhoA (K), and ROCK2 immunopositivities (OD values). Values are presented as the mean ± SD (n = 4). $*P < 0.05$, *vs.* control group; $\#P < 0.05$, *vs.* DEACMP group (one-way analysis of variance followed by the least significant difference test). DEACMP: Delayed encephalopathy after acute carbon monoxide poisoning; LINGO-1: leucine-rich repeat and immunoglobulin-like domain-containing protein-1; OD: optical density; RA: retinoic acid; RhoA: Ras homolog gene family member A; ROCK2: Rho-associated coiled-coil containing protein kinase 2.

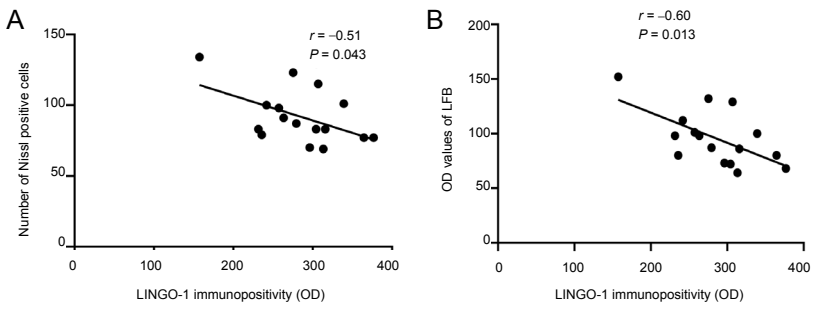

Figure 4 Correlation analyses between pathological changes observed at the lateral geniculate bodies or hippocampal regions and LINGO-1 protein levels in the lateral geniculate bodies.

(A) The correlation between the number of Nissl-positive cells and LINGO-1 immunopositivity (n = 16, r = –0.51, P = 0.043). (B) The correlation between the OD values for LFB staining and LINGO-1 immunopositivity (n = 16, r = –0.60, P = 0.013). The correlation was analyzed by the Spearman test. LINGO-1: Leucine-rich repeat and immunoglobulin-like domain-containing protein-1; LFB: Luxol fast blue; OD: optical density.

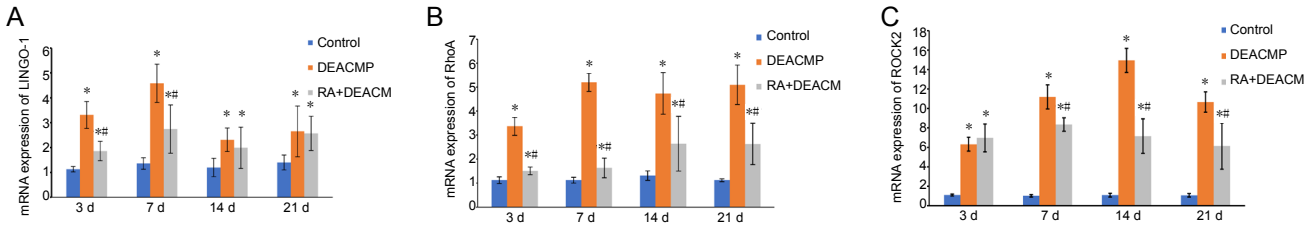

Figure 5 Gene expression levels for LINGO-1 and the RhoA/ROCK2 signaling pathway in whole-brain samples from DEACMP rats.

(A–C) Quantitative results of LINGO-1, RhoA, and ROCK2 mRNA expression (OD ratio to GAPDH). Data are presented as the mean ± SD (n = 4). $*P < 0.05$, *vs.* control group; $\#P < 0.05$, *vs.* DEACMP group (one-way analysis of variance followed by the least significant difference test). DEACMP: Delayed encephalopathy after acute carbon monoxide poisoning; GAPDH: glyceraldehyde 3-phosphate dehydrogenase; LINGO-1: leucine-rich repeat and immunoglobulin-like domain-containing protein-1; OD: optical density; RA: retinoic acid; RhoA: Ras homolog gene family member A; ROCK2: Rho-associated coiled-coil containing protein kinase 2.

poisoning was also analyzed. The increased expression level of Lingo-1 protein was correlated with more severe myelin regeneration damage and a reduction in Nissl-positive cells.

The results of the study by Xu et al. (2013) indicated that Lingo-1 is immediately upregulated in the white matter of rat brains, following acute CO poisoning, and exhibits regular secondary upregulation changes, which are positively correlated with white matter demyelination. The results of the current study revealed that the mRNA and protein expression levels of Lingo-1, RhoA, and Rock2 were significantly increased in the DEACMP group com-pared with those in the control group, at various time points, and that the expression gradually increased with time at 3–7 days or 7–14 days, before slowly decreasing after 14 or 21 days. This result indicates that CO poisoning can activate Lingo-1 expression and the RhoA/Rock2 signaling pathway and suggests that the Lingo-1 and the RhoA/Rock2 signaling pathway may participate in the pathophysiology of DEACMP, resulting in extensive white matter demyelination and neuronal necrosis and apoptosis.

RA is a vitamin A derivative that can penetrate the blood-brain barrier. RA forms an RA-RA receptor β complex by binding to the transcription factor RA receptor β, which then binds to a response element, located on the Lingo-1 promoter. Transcription inhibits the activation of the Lingo-1 myelin-dependent gene and, thus, reduces the activity of RhoA (Puttagunta et al., 2011). During the present study, we observed that the mRNA and protein expression levels of Lingo-1, RhoA, and Rock2 decreased in DEACMP rats treated with RA. In addition, the expression levels gradually increased at 7 or 14 days, before slowly decreasing with time after 14 or 21 days. The mean water maze latency was significantly lower in DEACMP rats following RA treatment. The hematoxylin and eosin staining results indicated that only a few neurons underwent apoptosis and necrosis in the DEACMP rats that received RA treatment. In addition, the disappearance of Nissl bodies was only observed in a few neurons, and the myelin sheath staining did not show the swelling or discontinuation of the myelin sheath, and no demyelination lesions were observed in DEACMP rats treated with RA. These results suggested that RA inhibits Lingo-1 expression, resulting in the reduced activation of the RhoA/Rock2 signaling pathway. However, in this study, we did not consider the results of phosphorylation, which is a limitation. Our results agree with those reported by Puttagunta and Di Giovanni (2011), who demonstrated that RA can inhibit the expression of Lingo-1. Reduced Lingo-1 expression promotes oligodendrocyte myelination, axonal growth, and neuron survival, alleviating DEACMP-induced brain damage (Mi et al., 2013). Therefore, RA may have therapeutic effects on DEACMP-induced brain damage.

In this study, we performed a preliminary analysis of the regulatory mechanisms associated with Lingo-1 and the RhoA/Rock2 signaling pathway during DEACMP-induced brain damage. The research method was relatively simple, however, and the research content is not sufficiently thorough or comprehensive; therefore, the clinical applicability of the conclusions of this study must be further validated. In the future, improvements in the screening process and the design of the research contents and methods must be implemented. Other areas of focus in future experiments will include the targets of Lingo-1 and RhoA/Rock2 signaling pathway activation and the pathophysiological mechanisms associated with DEACMP-induced brain injury, with a focus on the development of novel therapies. Despite the use of the phrase "activation of the RhoA/Rock2 signaling pathway", downstream effectors were not evaluated and the phosphorylation status (a classic marker of activation) was not explored, which is a limitation of this article. Future studies should examine the direct activation of the RhoA/Rock2 signaling pathway in response to Lingo-1.

From the current results, we concluded that Lingo-1 activates the RhoA/Rock2 signaling pathway, to promote DEACMP-induced brain damage, which could be an important pathophysiological mechanism underlying DEACMP. In addition, RA alleviated DEACMP-induced brain damage by inhibiting the expression of Lingo-1. Therefore, RA may represent an effective therapeutic agent for the treatment of DEACMP-induced brain damage.

Author contributions: *Study design: ZRP; experimental implementation: YQH, FLH; statistical analysis: YQH, ALY; manuscript draft: YQH. All authors have read and approved the manuscript.*
Conflicts of interest: *All authors declare no conflicts of interest.*
Financial support: *The authors received no funding for the research reported in this paper.*
Institutional review board statement: *This study was reviewed and approved by the Medical Ethics Committee of Xiangya Hospital of Central South Hospital (approval No. 201612684) on December 26, 2016.*
Copyright license agreement: *The Copyright License Agreement has been signed by all authors before publication.*
Data sharing statement: *Datasets analyzed during the current study are available from the corresponding author on reasonable request.*
Plagiarism check: *Checked twice by iThenticate.*
Peer review: *Externally peer reviewed.*

References

Almutiri S, Berry M, Logan A, Ahmed Z (2018) Non-viral-mediated suppression of AMIGO3 promotes disinhibited NT3-mediated regeneration of spinal cord dorsal column axons. Sci Rep 8:10707.
Andrews JL, Fernandez-Enright F (2015) A decade from discovery to therapy: Lingo-1, the dark horse in neurological and psychiatric disorders. Neurosci Biobehav Rev 56:97-114.
Baldwin KT, Giger RJ (2015) Insights into the physiological role of CNS regeneration inhibitors. Front Mol Neurosci 8:23.
Beppu T (2014) The role of MR imaging in assessment of brain damage from carbon monoxide poisoning: a review of the literature. AJNR Am J Neuroradiol 35:625-631.
Betterman K, Patel S (2014) Neurologic complications of carbon monoxide intoxication. Handb Clin Neurol 120:971-979.
Dong S, Cai FF, Chen QL, Song YN, Sun Y, Wei B, Li XY, Hu YY, Liu P, Su SB (2018) Chinese herbal formula Fuzheng Huayu alleviates CCl(4)-induced liver fibrosis in rats: a transcriptomic and proteomic analysis. Acta Pharmacol Sin 39:930-941.
Haines BP, Rigby PW (2008) Expression of the Lingo/LERN gene family during mouse embryogenesis. Gene Expr Patterns 8:79-86.

Han ST, Bhopale VM, Thom SR (2007) Xanthine oxidoreductase and neurological sequelae of carbon monoxide poisoning. Toxicol Lett 170:111-115.

Hanf KJM, Arndt JW, Liu Y, Gong BJ, Rushe M, Sopko R, Massol R, Smith B, Gao Y, Dalkilic-Liddle I, Lee X, Mojta S, Shao Z, Mi S, Pepinsky RB (2020) Functional activity of anti-LINGO-1 antibody opicinumab requires target engagement at a secondary binding site. MAbs 12:1713648.

Heasman SJ, Ridley AJ (2008) Mammalian Rho GTPases: new insights into their functions from in vivo studies. Nat Rev Mol Cell Biol 9:690-701.

Hu H, Pan X, Wan Y, Zhang Q, Liang W (2011) Factors affecting the prognosis of patients with delayed encephalopathy after acute carbon monoxide poisoning. Am J Emerg Med 29:261-264.

Korol A, Taiyab A, West-Mays JA (2016) RhoA/ROCK signaling regulates TGFβ-induced epithelial-mesenchymal transition of lens epithelial cells through MRTF-A. Mol Med 22:713-723.

Lettow I, Hoffmann A, Burmeister HP, Toepper R (2018) Delayed neuropsychological sequelae after carbon monoxide poisoning. Fortschr Neurol Psychiatr 86:342-347.

Li L, Sun L, Qiu Y, Zhu W, Hu K, Mao J (2020) Protective effect of stachydrine against cerebral ischemia-reperfusion injury by reducing inflammation and apoptosis through P65 and JAK2/STAT3 signaling pathway. Front Pharmacol 11:64.

Liu F, Guo S, Lü B, Xia Q, Cao B, Chen C, Zhang B, Li X, Cheng Z, Wen J (2002) Establishment of delayed encephalopathy rat model of carbon monoxide poisoning. Zhonghua Yi Xue Za Zhi 82:1645-1648.

Lv J, Xu RX, Jiang XD, Lu X, Ke YQ, Cai YQ, Du MX, Hu C, Zou YX, Qin LS, Zeng YJ (2010) Passive immunization with LINGO-1 polyclonal antiserum afforded neuroprotection and promoted functional recovery in a rat model of spinal cord injury. Neuroimmunomodulation 17:270-278.

Ma T, Li B, Le Y, Xu Y, Wang F, Tian Y, Cai Q, Liu Z, Xiao L, Li H (2019) Demyelination contributes to depression comorbidity in a rat model of chronic epilepsy via dysregulation of Olig2/LINGO-1 and disturbance of calcium homeostasis. Exp Neurol 321:113034.

Mi S, Sandrock A, Miller RH (2008) LINGO-1 and its role in CNS repair. Int J Biochem Cell Biol 40:1971-1978.

Mi S, Pepinsky RB, Cadavid D (2013) Blocking LINGO-1 as a therapy to promote CNS repair: from concept to the clinic. CNS Drugs 27:493-503.

Puttagunta R, Di Giovanni S (2011) Retinoic acid signaling in axonal regeneration. Front Mol Neurosci 4:59.

Puttagunta R, Schmandke A, Floriddia E, Gaub P, Fomin N, Ghyselinck NB, Di Giovanni S (2011) RA-RAR-β counteracts myelin-dependent inhibition of neurite outgrowth via Lingo-1 repression. J Cell Biol 193:1147-1156.

Quan Y, Wu Y, Zhan Z, Yang Y, Chen X, Wu K, Yu M (2020) Inhibition of the leucine-rich repeat protein lingo-1 enhances RGC survival in optic nerve injury. Exp Ther Med 19:619-629.

Rose JJ, Wang L, Xu Q, McTiernan CF, Shiva S, Tejero J, Gladwin MT (2017) Carbon monoxide poisoning: pathogenesis, management, and future directions of therapy. Am J Respir Crit Care Med 195:596-606.

Sakata M, Yoshida A, Haga M (1983) Simple determination of carboxyhemoglobin by double wavelength spectrophotometry of absorbance difference and the comparison with gas chromatographic method. Forensic Sci Int 21:187-195.

Schwab ME (2002) Repairing the injured spinal cord. Science 295:1029-1031.

Sipos E, Kurunczi A, Kasza A, Horváth J, Felszeghy K, Laroche S, Toldi J, Párducz A, Penke B, Penke Z (2007) Beta-amyloid pathology in the entorhinal cortex of rats induces memory deficits: implications for Alzheimer's disease. Neuroscience 147:28-36.

Sun SW, Nishioka C, Labib W, Liang HF (2015) Axonal terminals exposed to Amyloid-β may not lead to pre-synaptic axonal damage. J Alzheimers Dis 45:1139-1148.

Sun SW, Liang HF, Mei J, Xu D, Shi WX (2014) In vivo diffusion tensor imaging of amyloid-β-induced white matter damage in mice. J Alzheimers Dis 38:93-101.

Thom SR, Bhopale VM, Fisher D, Zhang J, Gimotty P (2004) Delayed neuropathology after carbon monoxide poisoning is immune-mediated. Proc Natl Acad Sci U S A 101:13660-13665.

Turkseven CH, Buyukakilli B, Balli E, Yetkin D, Erdal ME, Yilmaz SG, Sahin L (2017) Effects of Huperzin-A on the beta-amyloid accumulation in the brain and skeletal muscle cells of a rat model for Alzheimer's disease. Life Sci 184:47-57.

Walker SE, Spencer GE, Necakov A, Carlone RL (2018) Identification and characterization of microRNAs during retinoic acid-induced regeneration of a molluscan central nervous system. Int J Mol Sci 19:2741.

Wang H, Cheng X, Yu H, Zhang X, Guan M, Zhao L, Liu Y, Linag Y, Luo Y, Zhao C (2019) Activation of GABAA receptors enhances the behavioral recovery but not axonal sprouting in ischemic rats. Restor Neurol Neurosci 37:315-331.

Weaver LK (2009) Clinical practice. Carbon monoxide poisoning. N Engl J Med 360:1217-1225.

Wu D, Tang X, Gu LH, Li XL, Qi XY, Bai F, Chen XC, Wang JZ, Ren QG, Zhang ZJ (2018) LINGO-1 antibody ameliorates myelin impairment and spatial memory deficits in the early stage of 5XFAD mice. CNS Neurosci Ther 24:381-393.

Xing HY, Meng EY, Xia YP, Peng H (2015) Effect of retinoic acid on expression of LINGO-1 and neural regeneration after cerebral ischemia. J Huazhong Univ Sci Technolog Med Sci 35:54-57.

Xu XB, Liu XJ, Li JH, Wang XC, Lan HB, Ma HJ, Shi JX (2013) Dynamic expression of LINGO-1 in the cerebral white matter of rats after acute CO-poisoning. Linchuang Jizhen Zazhi 14:269-272.

Xue L, Wang WL, Li Y, Gong X, Bao JX, Zhang HJ, Xie XP, Chang YM, Li JS (2017) Effects of hyperbaric oxygen on hippocampal neuronal apoptosis in rats with acute carbon monoxide poisoning. Undersea Hyperb Med 44:121-131.

Yanagiha K, Ishii K, Tamaoka A (2017) Acetylcholinesterase inhibitor treatment alleviated cognitive impairment caused by delayed encephalopathy due to carbon monoxide poisoning: Two case reports and a review of the literature. Medicine (Baltimore) 96:e6125.

Yang T, Zhao K, Shu H, Chen X, Cheng J, Li S, Zhao Z, Kuang Y, Yu S (2017) The Nogo receptor inhibits proliferation, migration and axonal extension by transcriptionally regulating WNK1 in PC12 cells. Neuroreport 28:533-539.

Youssef AEH, Dief AE, El Azhary NM, Abdelmonsif DA, El-Fetiany OS (2019) LINGO-1 siRNA nanoparticles promote central remyelination in ethidium bromide-induced demyelination in rats. J Physiol Biochem 75:89-99.

Yu JZ, Ding J, Ma CG, Sun CH, Sun YF, Lu CZ, Xiao BG (2010) Therapeutic potential of experimental autoimmune encephalomyelitis by Fasudil, a Rho kinase inhibitor. J Neurosci Res 88:1664-1672.

Zhao N, Liang P, Zhuo X, Su C, Zong X, Guo B, Han D, Yan X, Hu S, Zhang Q, Tie X (2018) After treatment with methylene blue is effective against delayed encephalopathy after acute carbon monoxide poisoning. Basic Clin Pharmacol Toxicol 122:470-480.

C-Editor: Zhao M; S-Editors: Yu J, Li CH; L-Editors: Giles L, Yu J, Song LP; T-Editor: Jia Y